Pretransitional Structural Changes in the Thermal Denaturation of Ribonuclease S and S Protein

Simona D. Stelea and Timothy A. Keiderling
Department of Chemistry, University of Illinois at Chicago, 845 W. Taylor St., Chicago, Illinois 60607-7061 USA

ABSTRACT Two mechanisms have been proposed for the thermal unfolding of ribonuclease S (RNase S). The first is a sequential partial unfolding of the S peptide/S protein complex followed by dissociation, whereas the second is a concerted denaturation/dissociation. The thermal denaturation of ribonuclease S and its fragment, the S protein, were followed with circular dichroism and infrared spectra. These spectra were analyzed by the principal component method of factor analysis. The use of multiple spectral techniques and of factor analysis monitored different aspects of the denaturation simultaneously. The unfolding pathway was compared with that of the parent enzyme ribonuclease A (RNase A), and a model was devised to assess the importance of the dissociation in the unfolding. The unfolding patterns obtained from the melting curves of each protein imply the existence of multiple intermediate states and/or processes. Our data provide evidence that the pretransition in the unfolding of ribonuclease S is due to partial unfolding of the S protein/S peptide complex and that the dissociation occurs at higher temperature. Our observations are consistent with a sequential denaturation mechanism in which at least one partial unfolding step comes before the main conformational transition, which is instead a concerted, final unfolding/dissociation step.

INTRODUCTION

Ribonuclease S (Fig. 1) is the product of mild digestion of ribonuclease A by the bacterial protease subtilisin, the peptide bond scission occurring preferentially between residues 20 and 21 situated in the loop, which connects helices I and II (Richards and Vithayathil, 1959). Except for the region near the cleavage site, the two proteins, ribonuclease (RNase) A and S, have nearly identical three-dimensional structures, but small displacements exist in several loop regions (residues 36–39, 66–69, 88–96, and 110–114) and some β-sheet segments (Kim et al., 1992; Vadarajan and Richards, 1992; Wyckoff et al., 1970). However, the peptide bond scission significantly affects the stability of RNase S, which becomes more susceptible to hydrogen exchange (Haris et al., 1986) and, as shown by previous studies (Catazano et al., 1996) as well as by the present work, it has a melting point ~12°C lower than RNase A. The fragments resulting from the proteolysis, denoted as the S-peptide (residues 1–20) and the S-protein (residues 21–124), remain bound under native conditions, and the complex retains enzymatic activity. They can be separated at low pH, after which neither fragment has enzymatic activity.

Although S peptide (residues 1–20) has a highly fluctuating structure in solution with a dominant random coil conformation (Klee, 1968), once bound to S protein (residues 21–124), it forms a 10-residue long helix, denoted helix I. S peptide is anchored to the S protein by hydrogen bonds involving residues 11 to 14, which form the C terminus of helix I, and residues 44 to 48, which belong to a small β-strand of S protein (PDB entry 1rnu). In addition, a hydrogen bond between Arg-10 and Arg-33 and the burial of the hydrophobic residues Phe-8 and Met-13 stabilize the complex (Goldberg and Baldwin, 1998; Goldberg et al., 1997; Hearn et al., 1971; Vadarajan and Richards, 1992).

The structure of S protein has not been solved by x-ray crystallography or by nuclear magnetic resonance due to aggregation-related problems (Chakshusmati et al., 1999). However, the Stokes radius of just the S protein is very similar to that of RNase A, and its thermal denaturation has a much lower ΔC_p than would be calculated for the S protein based on the coordinates for its sequence in the RNase S structure. Both of these suggest that free S protein has a less compact structure than when bound to S peptide and lead to the proposal that the dissociation occurs with loss of S protein tertiary structure (Shindo et al., 1979).

Two mechanisms have been proposed for the equilibrium thermal unfolding of RNase S at neutral pH. The first one (Labhardt, 1981) is based on spectroscopic studies and consists of two competing pathways, as shown in Scheme 1. The top one is favored at protein concentrations higher than 50 μM, above which the melting temperature of RNase S also remains constant, and the bottom pathway is favored at lower concentrations.

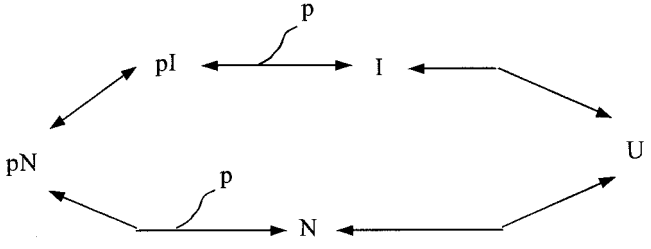

(1)

Submitted March 29, 2002, and accepted for publication May 24, 2002.

Address reprint requests to Timothy A. Keiderling, Department of Chemistry, University of Illinois at Chicago, 845 W. Taylor St., Chicago, IL 60607-7061. Tel.: 312-996-3156; Fax: 312-996-0431; E-mail: tak@uic.edu.

0006-3495/02/10/2259/11 $2.00

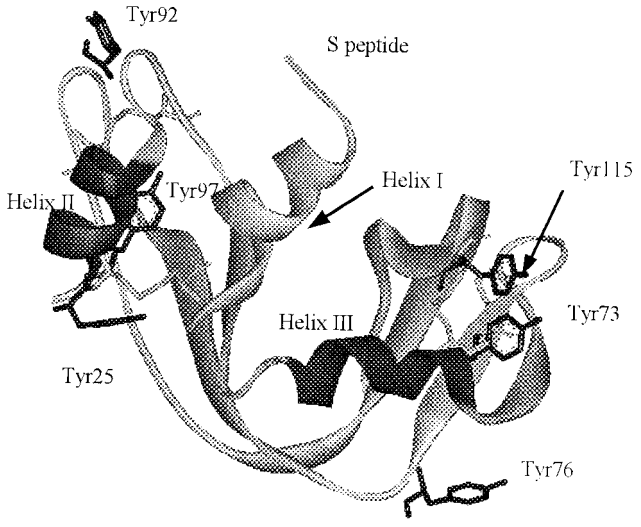

FIGURE 1 Ribbon diagram of RNase S (fragment 16–23 missing) showing the three helical segments and the position of the six tyrosines and the four disulfide bonds (PDB entry 1RNU).

The symbols represent: pN, native RNase S; N, native S protein; p, S peptide in any form; pI, partly unfolded, nondissociated intermediate; I, partly unfolded S protein; U, unfolded S protein.

Older calorimetry studies (Hearn et al., 1971) also suggest that the thermal denaturation of RNase S is not two-state. Additionally, kinetic folding/refolding intermediates have been observed in which the two fragments are bound, but the complex is partly unfolded (Labhardt and Baldwin, 1979; Schreier and Baldwin, 1976, 1977).

The second mechanism was derived from differential scanning calorimetry experiments and involves the simultaneous denaturation and dissociation of RNase S (Scheme 2) (Catazano et al., 1996):

$$\mathrm{pN} \rightleftarrows \mathrm{U} + \mathrm{p} \qquad (2)$$

where the same notation as Scheme 1 is used

In this work, the equilibrium thermal denaturation of RNase S and S protein at neutral pH was studied by electronic circular dichroism and by Fourier Transform infrared (FTIR) spectroscopy with the purpose of gaining new insight into the mechanism of unfolding of RNase S. Similar results regarding the denaturation of RNase A were previously published (Stelea et al., 2001) and are selectively used here for comparison. Our results are consistent with both RNase S and S protein undergoing multistate thermal transitions. Pretransitional changes in RNase S mostly involve helical regions, whereas the β-sheet is less affected. In RNase S, these changes consist of relatively localized structural modifications, little dissociation occurring before the main transition. S protein undergoes a broad thermal transition with a low degree of cooperativity, with one or more significantly populated intermediates. Our results also suggest that all three proteins have residual secondary structure in their thermally denaturated states.

MATERIALS AND METHODS

Protease-free bovine pancreas RNase A (type XIIA), RNase S (type XIIS), S protein (type XIIPR) were purchased from Sigma (St. Louis, MO) and S peptide from Biozyme Laboratories International (San Diego, CA).

The circular dichroism (CD) experiments were run on a JASCO J600 spectrometer at 2-nm bandwidth and with a 2-s time constant. Each spectrum was an average of 10 scans recorded at 20 nm/min. Cylindrical quartz cells with path lengths of 0.1 and 5 mm were used in the far-ultraviolet (UV) and the near-UV regions, respectively, to contain 1.5 mg/mL protein solutions prepared in 10 mM phosphate buffer (pH 6.8). The concentrations used in calculating the molar ellipticities were determined spectroscopically using the following extinction coefficients: RNase S $\epsilon_{277.5} = 9800\ \mathrm{M^{-1}\ cm^{-1}}$ (Catazano et al., 1996; Kurapkat et al., 1997; Sela and Anfinsen, 1957); S protein $\epsilon_{280} = 9055\ \mathrm{M^{-1}\ cm^{-1}}$ (Gilmanshin et al., 1996); S peptide $\epsilon_{258} = 299\ \mathrm{M^{-1}\ cm^{-1}}$ (Gilmanshin et al., 1996). The temperature was controlled using a Fischer Scientific circulating bath and monitored via a calibration curve.

Due to the necessity to keep the absorbance in the far-UV as low as possible, we limited the concentration to 1.5 mg/mL, which corresponds to approximately 100 μM. This concentration is within the limits at which the intermediate proposed by the first mechanism accumulates (Labhardt, 1981), but it has no relevance for the second mechanism, which is not concentration dependent. The melting point (T_m) of the main transition of RNase S was 46°C, the same as that observed by Labhardt in this concentration range.

For the FTIR experiments, ~5.5 mg/mL solutions of previously deuterium exchanged and lyophilized proteins were prepared in 10 mM deuterated phosphate buffer (apparent pD 6.8). The samples were sandwiched between two CaF_2 windows separated by a 50-μm Teflon spacer and held in a homemade thermostatted brass cell holder (Wang, 1993). The sample temperature was controlled by a Neslab RTE 110 circulating bath, and, after each change, 10 to 15 min were allowed for thermal equilibration of the cell. FTIR spectra were accumulated as the average of 512 scans/spectrum at 4 $\mathrm{cm^{-1}}$ nominal resolution using a Digilab FTS-60 spectrometer equipped either with a liquid-nitrogen cooled mercury cadmium telluride detector or a deuterated triglycine sulfate detector, depending on conditions, and continuously purged with dry air. Solvent correction of the protein spectra was performed by variable subtraction of buffer spectra, recorded under the same conditions, to obtain an approximately flat baseline between 1700 and 1900 $\mathrm{cm^{-1}}$. Correction for water vapor absorption was done by variable subtraction of a water vapor spectrum to eliminate all sharp features in the amide I′ region. The corrected FTIR spectra were truncated to the amide I′ region for analysis.

The mathematical analysis of the spectral sets, based on the principal component method of factor analysis (PC/FA) (Malinowski, 1991), was described in detail elsewhere (Pancoska et al., 1991, Stelea et al., 2001). Here, we provide only a brief summary. Using PC/FA, the CD and amide I′ FTIR temperature-dependent spectra, $\Theta_i(\nu)$ ($i = 1$ to n), over a spectral range from ν_1 to ν_2, for n temperatures, were decomposed into linear combinations of orthogonal, independent principal (nonnoise) components, $\phi_j(\nu)$, $j = 1$ to p. The overall loading, C_{ij}, of each spectral component was divided into an intensity (norm, N_i) and a bandshape (reduced loading, C_{ij}^r) component whose temperature dependencies characterize the thermal unfolding (Eq. 3).

$$\Theta_i(\nu) = \sum_{j=1}^{p} C_{ij}\phi(\nu) = N_i \sum_{j=1}^{p} C_{ij}\phi_j(\nu) \qquad (3)$$

The norms were calculated according to Eq. 4:

$$N_i = \sqrt{\int_{\nu_1}^{\nu_2} \Theta_i^2(\nu)d\nu} \quad (4)$$

and the reduced loadings are given by Eq. 5:

$$C_{ij}^r = C_{ij}/N_i \quad (5)$$

The denaturation curves were fitted to a sigmoidal, a sum of a linear and a sigmoidal, or a sum of two sigmoidal functions to probe the two-state versus multiple-state models. In some of the reduced loading, C_{ij}^r, and norm, N_i, curves, the pretransitional, and the main transition changes occur in the opposite sense, as a consequence of the area under the spectrum, represented by the norm N_i, decreasing and then increasing with temperature. Thus, these curves appear to have a minimum rather than the expected sigmoidal shape. These problems do not affect the original loadings, except for C_{i1} in the FTIR of S protein (see Discussion). To allow comparison between all the curves originating in the same set of spectra, one side of these curves was reflected through a horizontal line at the point of minimum, resulting in a conventional sigmoidal shape.

In addition to full bandshape analysis, the FTIR spectra were divided into two regions based on the appearance of the difference spectra ($\Theta(t) - \Theta(t_0)$, in which t_0 is the lowest temperature measured), each region being, in turn, separately analyzed by PC/FA. The two resulting regions roughly correspond to β-sheets (the region below 1640 cm^{-1}) and to helices and less well-defined structures (turns, loops, coil, the region above 1640 cm^{-1}).

The pretransitional changes observed in the thermal denaturation of RNase A (Stelea et al., 2001) were most prominent in the far-UV CD spectra and thus most likely occurred in the helical regions. This, together with the structural and spectral similarity between the two proteins, suggested a model for analysis of the denaturation of RNase S, which would allow one to assess the role of the dissociation in the pretransition. According to this model, the system is treated as a mixture of dissociated and nondissociated RNase S, in which the dissociated RNase S is represented as S protein and S peptide in a 1:1 mole ratio and the nondissociated RNase S as RNase A at that temperature. This model emphasizes mainly the temperature dependence of the dissociation, because most of the structural changes in the nondissociated complex are encompassed in the temperature dependence of the RNase A spectra, which display a similar pretransition. The RNase S spectra at each temperature were fit to Eq. 6:

$$\Theta^{RS}(T) = \alpha*(\Theta^{SP}(T) + \Theta^{P}(T)) + (1 - \alpha)*\Theta^{RA}(T) \quad (6)$$

in which $\Theta^{RS}(T)$, $\Theta^{SP}(T)$, $\Theta^{P}(T)$, and $\Theta^{RA}(T)$ represent the concentration corrected spectra of RNase S, S protein, S peptide, and RNase A at a given temperature, T, and α is the fitting parameter.

For structural comparison of RNase S and S protein, their low temperature far-UV CD and FTIR spectra were used to predict the fractional secondary structure content of the native states of the two proteins. We used our restricted multiple regression algorithm in addition to PC/FA (PC/FA restricted multiple regression) following methods that have been described in detail elsewhere (Baumruk et al., 1996; Pancoska et al., 1991, 1994, 1995).

RESULTS

Three sets of spectra (near-UV CD, far-UV CD, and FTIR) each for RNase S and S protein are presented in Fig. 2, *a* through *f*. The main transition of RNase S occurs between ~36°C and 55°C in dilute solution as monitored with near- and far-UV CD and between ~40°C and 63°C in more concentrated solutions in D_2O as monitored with FTIR. Small pretransitional changes are observed in the far-UV CD and FTIR sets. Similar trends are observed in the spectral sets of S protein, but the main transitions are more gradual and occur at lower temperature (~18°C-50°C in near- and far-UV CD and ~26°C-58°C in FTIR). No isosbestic points appear in the FTIR spectra of either protein.

To see better the effect on the spectra of the scission of the peptide bond in RNase A to form RNase S and of the removal of S peptide from the RNase S to form S protein, the native state spectra of RNase S and S protein in near- and far-UV CD are compared with those of RNase A (Fig. 3, *a* and *b*). In Fig. 3 *c*, the far-UV CD spectra of these proteins when thermally denatured are presented to provide insight with respect to the residual secondary structure of the thermally unfolded proteins.

As seen in Fig. 3 *a*, some bandshape (loss of the 289-nm shoulder and a small blue shift) and especially intensity differences can be observed between the near-UV CD spectra of RNase A (trace 1) and RNase S (trace 2). The intensity change induced by the proteolysis is larger in the longer wavelength region, which is dominated by the Tyr contributions. The removal of the S peptide further decreases the intensity in the near-UV, and a further blue shift of the maximum by approximately 1 to 1.5 nm is observed (traces 2 and 3). It should be noted that, with the exception of Phe-8 (Phe contributions to the near UV CD have been calculated to be negligible (Kurapkat et al., 1997)), all three proteins contain the same aromatic residues and disulfides.

Except for a small blue shift below 200 nm, the native state far-UV CD spectra of RNase S and A are very similar (Fig. 3 *b*, compare traces 1 and 2). The removal of S peptide from RNase S to form S protein produces a large decrease in $\Delta\epsilon$ (Fig. 3 *b*, traces 2 and 3). However, there is a significant residual CD intensity in the 200- to 230-nm region for the thermally denatured proteins (Fig. 3 *c*). In fact, the loss of CD intensity in this region on going from RNase S (trace 2) to S protein (trace 3) is larger than the loss of CD here on thermal denaturation of S protein (compare Fig. 3 *b*, traces 3 and 4). Of course, the change beyond 200 nm, where the coil form has a significant contribution, is greater on denaturation. The high temperature far-UV CD spectra of all three proteins (Fig. 3 *c*) are almost identical in shape, but there is a loss in intensity for the sum of the S protein (trace 3) and S peptide (trace 4) CD as compared with that of thermally dissociated RNase S (trace 2).

As found in the far-UV CD, the FTIR amide I′ spectra of RNase S and RNase A (not shown) are almost identical, which would be expected from the structural similarity of the two proteins. However, the ratio of the extinction coefficients of RNase S and S protein at 1635 cm^{-1} (~1.2), a frequency typically assigned to β-sheet, is unexpectedly close to the same ratio at 1652 cm^{-1} (~1.3), which typically corresponds to α-helix.

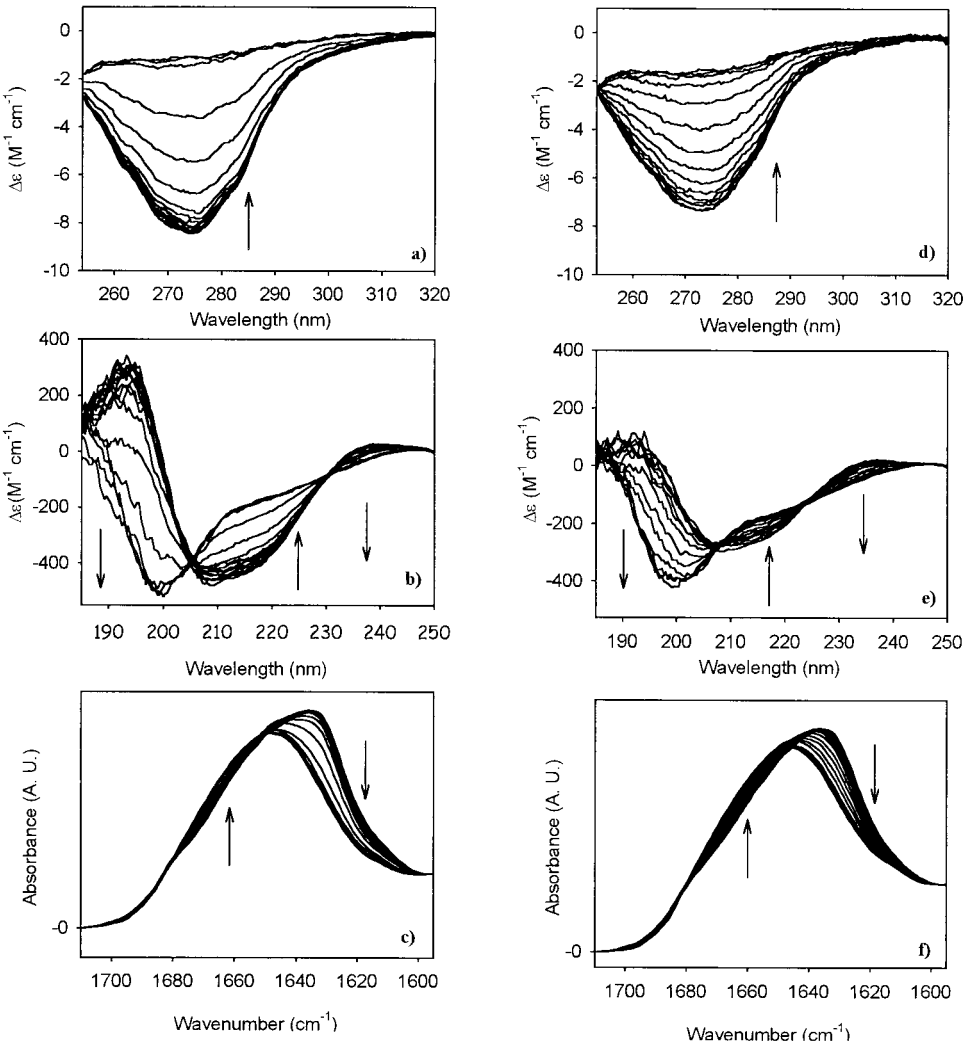

FIGURE 2 Thermal dependence of the spectra of RNase S: (*a*) near-UV CD, (*b*) far-UV CD, and (*c*) FTIR and of S protein: (*d*) near-UV CD, (*e*) far-UV CD, and (*f*) FTIR. The arrows show the direction of change with increasing temperature.

Each set of spectra was analyzed by the principal component method of factor analysis (PC/FA, see Materials and Methods) (Malinowski, 1991) to obtain several orthogonal, temperature-independent spectral components (ϕ_i) and their loadings (C_{ij}) whose temperature dependencies can be used to characterize the thermal unfolding. In all the cases, two components were sufficient to reproduce better than 99% of the spectral bandshape (Fig. 4, *a* through *f*). Each overall loading was additionally parsed into an intensity (norm N_i) and a bandshape component (C_{ij}^r), but these are not presented here because they do not provide any significant new insights at this point beyond the observations we previously made for RNase A (Stelea et al., 2001).

Because all spectral components (ϕ_i) describe features of the same spectra, it is expected that in a two-state denaturation all their loadings would have overlapping temperature dependencies. However, as Fig. 4 illustrates, whereas the curves obtained from different loadings for near-UV CD do overlap, those for far-UV CD and FTIR do not, suggesting that, with these two structural monitors, the two components monitor either different thermally induced changes (for example, dissociation and structural modifications) or the unfolding of different parts of the molecule, or both. For RNase S, the curves C_{i1} and C_{i2} for far-UV CD and amide I′ FTIR show differences in sensitivities to the pretransition, and the different techniques sense the main transition differently. For S protein, the pretransition difference between C_{i1} and C_{i2} curves disappears in far-UV CD, but the differences extend to the main transition and the resulting curves are more distorted from a sigmoidal shape in FTIR. The main transition of S protein, as monitored by different sets of loadings, is broader, less cooperative, and has a lower melting temperature than the corresponding transition of RNase S.

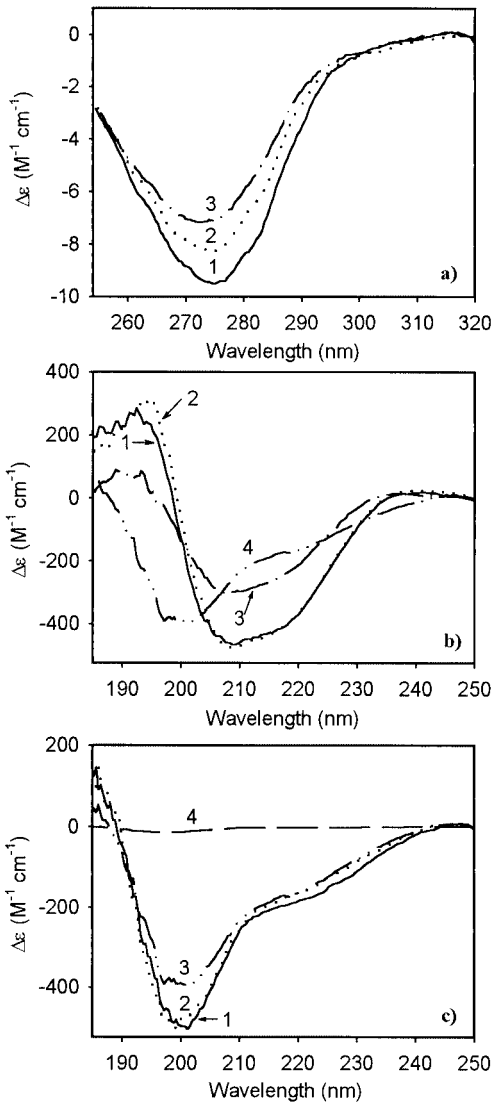

FIGURE 3 Comparison between the CD spectra of RNase A, RNase S, and S protein. (*a*) Near-UV CD: RNase A at 5°C (trace 1, —); RNase S at 4°C (trace 2, ...); and S protein at 5°C (trace 3, −·−). (*b*) Far-UV CD: RNase A at 5°C (trace 1, —); RNase S at 4°C (trace 2, ...); S protein at 5°C (trace 3, −·−), and S protein at 58°C (trace 4, −··−). (c) Denatured state spectra of RNase A at 78°C (trace 1, —); RNase S at 63°C (trace 2, ...); S protein at 58°C (trace 3, −·−); and S peptide at 58°C (trace 4, − −). All the spectra are expressed as $\Delta\epsilon$ (M^{-1} cm^{-1}), where the molarity M refers to the molarity of the protein.

As monitored by the near-UV CD C_{i1} and C_{i2} (Fig. 4 *a*), the tertiary structure of RNase S starts unfolding at ~37°C, ends around 52°C (T_m 46°C), and appears to be a cooperative two-state process because the transition is relatively sharp, and the two curves overlap closely. For the S protein (Fig. 4 *d*), a similar, but broader transition is observed with $T_m \sim 36$°C.

In the secondary structure dominated far-UV CD (Fig. 4 *b*), the RNase S C_{i2} displays the same characteristics as do the near-UV CD C_{ij}, whereas C_{i1} shows a pretransition similar to the one observed in the far-UV CD of RNase A (Stelea et al., 2001). Similar to RNase A, the pattern of the norm, N_i, or overall intensity variable versus T follows the temperature dependence of the C_{i1} component, whereas the corresponding bandshape changes (C_{i1}^r) occur at higher temperatures and match closely the bandshape transitions in the near-UV CD. This would be consistent with the loss of some helix in the pretransition, because helix is the dominant contribution to the far-UV CD intensity (reflected in the norm and C_{i1}) and a partial loss would not significantly alter the bandshape (C_{i1}^r).

By contrast, the S protein as monitored with far-UV CD (Fig. 4 *e*) appears to have a single, although broad, transition directly following that seen in the near-UV CD. However, the two spectral components, C_{i1} and C_{i2}, do have slightly different T_m values, suggesting a more complex mechanism underlying the secondary structure transition.

In FTIR (Fig. 4 *c*), RNase S shows a clear pretransition in C_{i2}, the spectral component reflecting a band shift, but evidences little in C_{i1}, the component most sensitive to the overall intensity. Upon decomposition of the loadings, the small low temperature changes observed in the RNase S spectra appear in the bandshape (C_{ij}^r) rather than in the intensity (N_i) curves as would be consistent with their dominating C_{i2}. Loss of a component of secondary structure could shift the IR band, but the effect on the integrated area or intensity is minimal.

The pretransitional region, as well as its T_m, is less clear in the FTIR unfolding curves of S protein. Whereas C_{i2} again shows a pretransition, its breadth coupled with that of the main transition almost obscures its detection. The S protein FTIR C_{i1} has a complex low temperature variation that in turn impacts the N_i, norm, curve because C_{i1} represents the bulk of the intensity.

When the high (>1640 cm^{-1}) and low frequency (<1640 cm^{-1}) regions of the amide I′ band of each protein were separately analyzed by factor analysis (results not shown), the pretransitional changes were larger for both proteins in the higher frequency region. The contributions to this spectral region arise mainly from helical and other structures (turns and bends). The pretransitional changes observed in the low frequency region occurred for both proteins mainly below 20°C where the C_{i1} curve is difficult to interpret.

The differences in the melting temperature observed between the FTIR and UV CD sets of each protein are in part due to deuteration effects (Makhatadze et al., 1995) and differences in the experimental conditions. (In the FTIR, the temperature was measured in the cell jacket, whereas in UV CD it was measured directly in the cell.) In addition, the FTIR experiments are run on samples of ~4 times higher concentration, which may affect the melting point (Catazano et al., 1996; Labhardt, 1981).

The temperature dependence of the parameter α, representing the degree of dissociation (see Materials and Meth-

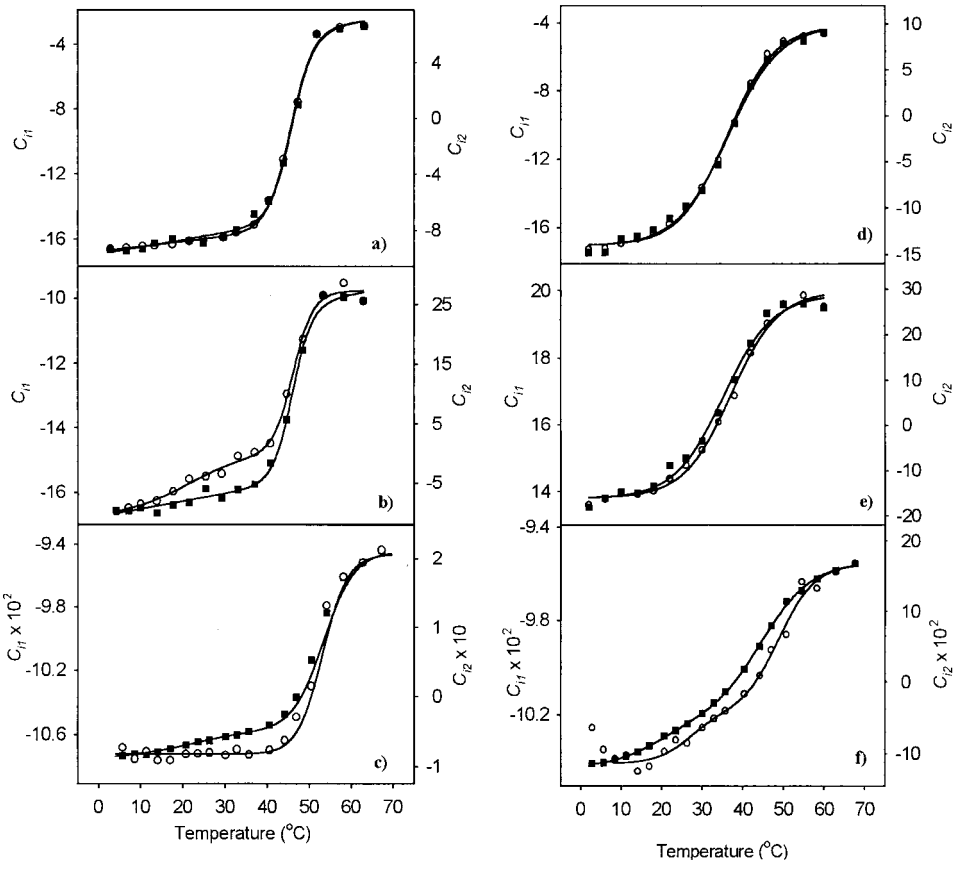

FIGURE 4 Temperature dependence of the loadings (C_{i1} (○) and C_{i2} (■)) obtained from the principal component factor analysis of different sets of spectra of RNase S: (*a*) near-UV CD, (*b*) far-UV CD, and (*c*) FTIR and of S protein: (*d*) near-UV CD, (*e*) far-UV CD, and (*f*) FTIR. The lines represent the regression curves from the following fitting of the loadings: (*a*) both loadings − line + sigmoid; (*b*) C_{i1} − double sigmoid, C_{i2} − line + sigmoid; (*c*) C_{i1} − single sigmoid, C_{i2} − double sigmoid; (*d*) both loadings − single sigmoid; (*e*) both loadings − single sigmoid; (*f*) both loadings − double sigmoid. The C_{i1} curve in *f* was mirror imaged about the data point at 30°C as explained in Materials and Methods. Also, the first two points in the C_{i1} curve (*f*) were considered outliers, and consequently, they were ignored in the fitting.

ods) obtained from fitting the RNase S far-UV CD spectra as a linear combination of RNase A, S protein, and S peptide spectra is presented in Fig. 5. The parameter is best fit to a combination of a linear and a sigmoidal function, and the resulting melting point is a couple of degrees higher than the T_m of the far-UV CD C_{ij} curves.

DISCUSSION

Structural considerations with respect to the native and denatured states of RNase S and S protein.

The similarity of the low temperature far-UV CD and FTIR spectra of RNase S and A (Fig. 3 *b*, c) is consistent with the similarity of the secondary structures of the two proteins as observed in the crystal (PDB entries 1RNU (RNase S) and 3RN3 (RNase A)) (Kim et al., 1992; Vadarajan and Richards, 1992; Wlodawer et al., 1982) and in the nuclear magnetic resonance solution structures (Rico et al., 1989).

The bandshape differences observed between the near-UV CD spectra of RNase S and A are small (consisting of a small blue shift and the loss of the shoulder at 289 nm, which may reflect the changes in the environment of Tyr-25 due to the peptide bond cleavage (Horwitz and Strickland, 1971)). However, more significant intensity differences are observed, being larger in the longer (Tyr-dominated) wavelength region. These intensity differences, not apparent in the far-UV CD, could be related to the increased internal motion of RNase S due to the strand cleavage, a property that also correlates with its lower thermal stability as compared with RNase A. Internal motion, expected to increase with lower stability of RNase S, samples a larger number of conformations, thus leading to more cancellation in the near UV CD as compared with RNase A. It can be noted that four of six Tyr residues and five of the eight Cys residues are situated either close to the cleavage point or close to those loops, which exhibit small structural differences between the two proteins (Vadarajan and Richards, 1992; Wlodawer

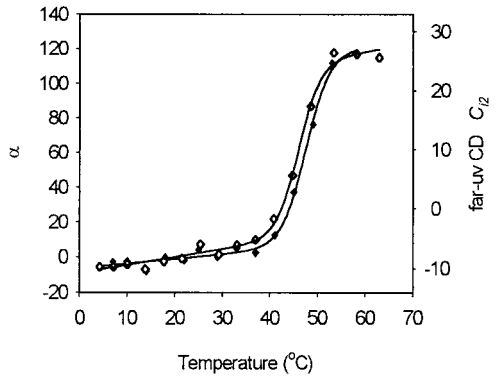

FIGURE 5 Temperature dependence of far-UV CD C_{i2} (◇) and of parameter α (◆) obtained from the fitting of the far-UV CD spectra of RNase S as a linear combination of spectra of RNase A, S protein, and S peptide at each temperature. Line + sigmoid regression.

et al., 1982). Thus, these near-UV probes may monitor different microenvironments in RNase S and A.

As previously mentioned, the structure of S protein has not yet been determined. There is evidence, though, that binding S peptide to S protein to form RNase S is accompanied by changes in the tertiary structure of S protein (Chakshusmati et al., 1999; Graziano et al., 1996; Shindo et al., 1979). Our data support the fact that the dissociation of the complex affects the tertiary structure and, in addition, suggest that the secondary structure of the S protein segment also changes in this dissociation process.

With the exception of Phe-8, all the residues that contribute to the near-UV CD ($\lambda > 250$ nm) are located on the S protein segment. Calculations of the various contributions to the near-UV CD spectra predict that the contribution of Phe is negligible (Goux and Hooker, 1980; Kurapkat et al., 1997). However, the low temperature near-UV CD spectra of RNase S and S protein show a rather large intensity difference (Fig. 3 *a*, traces 2 and 3). Modification of the environment of Tyr-25 due to the bond cleavage is already apparent in the spectrum of RNase S (Fig. 3 *a*). The remaining contributors to the CD of these proteins (tyrosines and disulfide bonds) are located in regions rather remote from the S peptide moiety and would be expected to be less affected if the removal of S peptide induced only local structural changes. As a consequence, the near-UV CD spectral change observed for S protein with respect to RNase S is consistent with there being more than local changes, i.e., affecting the whole molecule and presumably further relaxing the tertiary structure. Our data are consistent with a rather less compact structure of S protein relative to RNase S, as has been indicated by its large Stokes radius (Chakshusmati et al., 1999).

The loss of helix I is evident in the far-UV spectra of S protein as a loss of intensity as compared with RNase S (Fig. 3 *b*, traces 2 and 3), but the S protein spectra still retain a partial α-helical character. Using the restricted multiple

TABLE 1 Fraction of secondary structures of S protein and RNase S predicted by PC/FA RMR from far-UV CD and FTIR

	S Protein		RNase S	
	FC_α	FC_β	FC_α*	FC_β
Far-UV CD†	17	32	25	32
FTIR†	15	27	7	33
Far-UV CD‡	12	33	19	36
X-ray§	-	-	21	31.5

*FC_α is the total fraction of α- and 3_{10} helix.
†Present work. Fractions calculated from spectra at 2°C for S protein and 4°C for RNase S. Standard errors are of the order of 7% α-helix, 9% β-sheet for CD, and 13% α-helix, 8% β-sheet for FTIR with this method.
‡(Labhardt, 1982) Fractions calculated from spectra at 10°C for S protein and 32°C for RNase S.
§The x-ray values were taken from the Protein Data Bank (PDB 1RNU).

regression prediction method and our protein reference set (Baumruk et al., 1996; Pancoska et al., 1995), the fractional components (FC) of secondary structure in native S protein were calculated from both far-UV CD and FTIR spectra (Table 1). Both methods yielded very similar results. The average predicted FC_α (~16%) of S protein is in very good agreement with that which might be expected for S protein (16%), if the loss of helix I were the only loss of helical structure occurring upon dissociation.

In the case of β-sheet, the situation is different. The predicted FC_β (~30%) is significantly lower than the expected value (41%) calculated from the x-ray structure if one assumed that the removal of the S peptide residues were the only structural change. Similar values were obtained from far-UV CD by Labhardt, who also used a linear regression method but a different basis set of protein data (Labhardt, 1982) (Table 1). Although the average errors calculated from the data base are relatively large (Table 1), the similarity of the FCs for S protein as predicted using two different techniques (far-UV CD and FTIR) and the agreement of the predicted FC_α to the expected value lead us believe that the 11% difference may have meaning beyond the inaccuracy of the prediction (whose normal error is 8%–9% for β-sheet). As a test, the same calculations were run using the low temperature spectra of RNase S. Except for the FC_α calculated from FTIR, whose prediction was low by almost 14% (and is known to be much less accurate than CD for α-helix determination (Baello et al., 2000; Keiderling, 2000)), the rest of the calculated fractional components were within 4% of the accepted x-ray structure values (Table 1). Therefore, our data can be viewed as being consistent with the S protein part undergoing structural changes in β-sheet segments and preserving much of its remaining RNase S-like helical structure upon the release of S peptide. This result is also supported by the ratio of the FTIR molar extinction coefficients at 1635 cm^{-1}, $\varepsilon_{RNaseS}/\varepsilon_{Sprotein} \sim 1.2$. This would be expected to be significantly smaller than the same ratio at 1652 cm^{-1}, $\varepsilon_{RNaseS}/\varepsilon_{Sprotein} \sim 1.3$, if only loss of α-helix unaccompanied by loss of

β-strands occurred (see Results). Consistent with this interpretation, β-structure formation in S protein upon binding of S peptide was also proposed based on Raman difference spectroscopy (Gilmanshin et al., 1996). The β-strands most affected by the removal of S peptide are 43 to 47 and 116 to 124, which both have hydrophobic residues buried by the S peptide. Strand 43 to 47 also anchors the S peptide to S protein through H-bonds. These strands being short, modification of a few residues would tend to alter the β-sheet character of the whole strand.

Despite their structural differences, the shapes of the far-UV CD spectra for the three thermally denatured proteins, RNase A, RNase S, and S protein, are almost identical aside from lower intensity for the S protein (Fig. 3 *c*). Because there is evidence that the thermally denatured state of RNase A is a compact molecule (Sosnick and Trewhella, 1992) having residual secondary structure (Labhardt, 1982; Seshadri et al., 1994; Sosnick and Trewhella, 1992), these facts are reason to believe that the denatured RNase S, and S protein as well, retain secondary structure. The CD intensity at 200 nm in the RNase S spectrum (Fig. 3 *c*, trace 2) is larger than that of the sum of the intensities in the S protein (trace 3) and S peptide (trace 4) spectra at the same wavelength, but it is identical to that of the RNase A spectrum (trace 1). This suggests that the structure of the denatured RNase S is less disordered than the structure of the denatured separated segments and implies that some residual interactions exist between S peptide and S protein in their denatured states.

As shown in Fig. 3 *b*, the removal of the S peptide, which represents $\sim$⅓ of the helical content of RNaseS, produces a change in the region between 200 and 230 nm of the far-UV CD spectrum of RNase S (trace 2) approximately twice as large as the change induced in the same region of the spectrum of S protein by the thermal denaturation (traces 3 and 4). This fact could be interpreted in one of the following ways. First, if one assumes that the denatured S protein does not retain any secondary structure, the larger difference between traces 2 and 3 as compared with that between traces 3 and 4 means that the removal of S peptide determines, in addition to the loss of helix I, also a loss of secondary structure in the S protein segment. On the other hand, if the difference between the spectra of native RNase S and S protein represents only the loss of helix I, the thermally unfolded S protein must retain secondary structure, otherwise a larger signal decrease should be observed upon denaturation. A third possibility would be a combination of the previous two, in which S protein loses more secondary structure than helix I but also retains some in its denatured state. This third possibility is consistent with both the results of the secondary structure predictions and the resemblance of the high temperature bandshape of S protein to those of RNase A and RNase S.

Thermal transition of RNase S

The PC/FA whole bandshape analysis method demonstrates that there is clearly a pretransition region for both RNase S and S protein, but its detectability is technique dependent. The pretransition is certainly more pronounced for RNase S, whose behavior in this regard parallels earlier observations for RNase A (Stelea et al., 2001).

Pretransitional changes can be observed in the far-UV CD and, to a smaller extent, in the FTIR denaturation curves of RNase S, which suggests that they are due to the modification of the secondary structure, presumably involving loss of helix, the contribution of which dominates the far-UV CD. The structure of the intermediate is largely native-like because the changes seem to have very small effect on the tertiary structure as monitored with the near-UV CD. By contrast, the S protein transitions are nearly undetectable in the far-UV CD but are quite apparent in the FTIR spectra. The fact that the far-UV CD pretransition is so much more pronounced in the RNase S than in the S protein spectra suggests that it occurs, at least in part, in the helix I region (i.e., unwinding of helix I), which does not exist in S protein. Alternatively, it may occur in a region common to both proteins, but one that had already changed in S protein due to the removal of S peptide. As we have argued previously for RNase A (Stelea et al., 2001), in view of the lack of a near-UV pretransitional change, the far-UV change points toward the region neighboring helix II as the helical region common to both RNase S and S protein. The C terminus of helix II is likely to be affected by the removal of S peptide due to the breaking of the H-bond between Arg-33 and Arg-10.

The separate analysis of the two regions of the amide I′ (below and above 1640 cm^{-1}) for RNase S (not shown) shows a pretransitional change (between 13°C and 40°C) in the higher frequency region, which consists of contributions from helices and connecting structures like bends, turns, or loops. Although this analysis does not allow the quantification of the contribution from each type of structure, the far-UV CD results support the participation of at least one helical segment in the pretransition, as explained above. A small intensity modification is also noticed in the sheet region ($<$1640 cm^{-1}), but the bulk of the β-sheet structure must unfold during the main transition in a cooperative fashion similar to that seen in the main transition for the analysis of the whole bandshape.

Thermal transition of S protein

As reflected by the denaturation curves derived from all three spectral sets (Fig. 4, *d–f*), the thermal transition of S protein starts at a lower temperature and has lower melting points than does the transition of RNase S, reflecting its lower stability.

The modification of the tertiary structure is reflected as a broad sigmoidal transition in each of the near-UV CD thermal dependence curves (Fig. 4 *d*). This gradual variation behavior, similar to that previously obtained using circular dichroism, optical rotation, or absorption at a single frequency in the near-UV region (Sherwood and Potts, 1965; Simons et al., 1969), suggests a gradual, multistate thermal denaturation with significantly populated macroscopic state intermediates (Lumry et al., 1966). Similar broad thermal denaturation curves were obtained here from full bandshape analysis of the far-UV CD (Fig. 4 *e*). However, the FTIR curves are better represented by double sigmoid functions, and the two loadings do not overlap, showing clearer evidence of a multistate transition (Fig. 4 *f*). The low-temperature behavior of the FTIR C_{i1} is rather unusual, the curve displaying a minimum at ~26°C. To obtain the conventional sigmoidal shape for comparison with the other loadings, the low temperature portion of this curve was mirror imaged as explained in Materials and Methods. However, the main transition does not overlap with C_{i2}, whether regarded in the original or corrected form.

The analysis of the β-sheet region (<1640 cm^{-1}) of the amide I′ band of S protein (not shown) displayed the small pretransitional loss of intensity that was also observed for RNase S. The main transition starts ~10°C lower and is ~10°C broader than that of RNase S, showing a much lower cooperativity for the denaturation of the sheet component. However, the C_{i1} and C_{i2} curves again overlap well in the main transition region.

The analysis of the second amide I′ region of S protein (>1640 cm^{-1}), on the other hand, revealed two different trends. The C_{i1} curve corresponds to a very broad transition (~40°C wide) starting around 10°C and is indicative of a pretransition below 35°C followed by the main transition between 35°C and 50°C. The C_{i2} curve is sigmoidal, narrower than C_{i1} and follows the main transition that was identified in the low wave-number region. It is rather difficult to interpret these results, but the contribution of α-helices to the pretransition cannot be ruled out.

The disulfides and tyrosines are not evenly distributed throughout the whole molecule, but they rather form two groups, each comprising three Tyr residues and two disulfide bonds, one group on each side of the molecule, as seen in Fig. 1. Different methods were used for the calculation and analysis of the near-UV CD spectra of RNase S (Goux and Hooker, 1980; Horwitz and Strickland, 1971; Kurapkat et al., 1997; Strickland, 1972). Although all of the results point toward the three tyrosines on the four stranded side of the molecule (Tyr-73, Tyr-76, and Tyr-115) as major contributors to the near-UV CD, different results were obtained with respect to the contributing disulfides. However, the most recent study (Kurapkat et al., 1997), based on more elaborate models and on higher resolution crystal structures, suggest that the two cystines located on the same side as the above tyrosines (58–110 and 65–72) have a more important role. Assuming that this is also true for S protein, the near-UV CD spectra should be most sensitive to changes in the tertiary structure for this part of the molecule. Because the near-UV CD spectra do not sense the pretransition, it is therefore likely that any structures that are modified in this lower temperature range (Fig. 4 *f*) are situated in the portion of the molecule containing helix II, rather than in the region around helix III.

Mechanism of RNase S denaturation

The resemblance of the pretransitional regions of the far-UV CD denaturation curves of RNase A and S suggests that the intermediate state observed is a partly unfolded structure and it is not due to the dissociation of RNase S. As explained in the Materials and Methods section, we further tested this assumption by fitting of the far-UV spectra of RNase S to a linear combination of RNase A, S protein, and S peptide spectra. If one assumes that the conformational changes are the same in RNase A and nondissociated RNase S, the temperature dependence of the coefficient, α, as obtained from the fitting shows the involvement of the dissociation in each stage of the transition. The α curve (Fig. 5, filled symbols) shows no sigmoidal pretransition, the low temperature region having only a linear dependence. Although this method has some error due to the small differences between the low-, as well as the high-temperature spectra of RNase S and A, the point of the model is valid and it shows that the pretransition is determined by secondary structural changes and not by dissociation. The dissociation starts playing a role only above 40°C with the onset of the main transition. From this point on, the melting curves obtained from different loadings monitor three processes: the unfolding of the complex, the dissociation of the complex, and the unfolding of the S protein.

The parameter α reaches the middle of the transition at 48°C, which is a couple of degrees higher than the main transition in the C_{i1} and C_{i2} unfolding curves obtained from far-UV CD (46°C). (The C_{i2} unfolding curve (empty symbols) is shown in Fig. 5 for comparison.) This shows that, even in the main unfolding transition, the structural changes are more sensitive to temperature than is the dissociation.

RNase A is not a perfect model for the nondissociated RNase S in either the near-UV CD or FTIR due to the spectral differences between their low-temperature native state spectra, and/or different shapes of the denaturation curves in the pretransition region. Thus, some of the pretransitional changes monitored by these spectra exist in one protein but not in the other, and they are falsely compensated in the calculation by the parameter α.

To summarize, our data support the existence of a pretransitional intermediate in the thermal denaturation of RNase S, which was not observed in either of the two mentioned studies (Labhardt, 1981). The intermediate is a partly unfolded, native-like structure with modified helical

and, to a lesser extent, β-sheet elements. Under the conditions of our experiments, which fall within those of the upper branch of scheme 1, the unfolding mechanism of RNase S appears to be a stepwise mechanism. The first step of the unfolding consists of the conformational modification and destabilization of RNase S and occurs at temperatures below the main transition. However, the main transition seems to follow the second previously proposed mechanism in which the dissociation and conformational changes occur in parallel. Some accumulation of partly unfolded nondissociated species is possible during the main transition, because the conformational changes start at lower temperature and have a lower midtransition point than does the dissociation (Fig. 5). However, the pN $\rightleftharpoons$ pI reaction does not seem to be the major unfolding reaction proposed earlier (Labhardt, 1981) because the difference between the C_{i2} and α curves (Fig. 5) is not larger than 10% to 12%.

CONCLUSION

Our results confirm the decrease in stability induced in RNase A by the cleavage of the peptide bond, because the whole transition of RNase S is translated toward lower temperature. However, there are similarities in the denaturation of the two proteins: the helical segments of RNase S and A undergo parallel pretransitional changes, which do not have a remarkable effect on their tertiary structures. The pretransition of the β-sheet, on the other hand, occurs at a lower temperature and is more gradual in RNase S.

The intermediate state in the thermal unfolding of RNase S is due to losses of secondary structure, mainly helix and loops, but also small fragments of strands. Most of the β-sheet is stable and unfolds during the main transition in concert with the dissociation of the complex.

S protein also undergoes multistate thermal unfolding with observable pretransitions. The removal of the S peptide leads to the loss of β-sheet even in the native state of S protein, further decreasing the stability of the molecule and the cooperativity of the transition. The pretransitional changes affect mainly less structured segments (turns, loops, etc), possibly some helical residues, and are followed by a broad transition of the remaining structure. The molecule is more heterogeneous than RNase S from both structural and stability points of view.

Finally, our results show evidence that the denatured states of all three proteins retain some secondary structure and that there are residual interactions between the denatured S protein and S peptide.

This work was supported in part by a grant from the Research Corporation. Advice on data analysis from Dr. Petr Pancoska is gratefully acknowledged.

REFERENCES

Baello, B. I., P. Pancoska, and T. A. Keiderling. 2000. Enhanced prediction accuracy of protein secondary structure using hydrogen exchange FT-IR spectroscopy. *Anal. Biochem.* 280:46–57.

Baumruk, V., P. Pancoska, and T. A. Keiderling. 1996. Predictions of secondary structure using statistical analyses of electronic and vibrational circular dichroism and Fourier transform infrared spectra of proteins in H_2O. *J. Mol. Biol.* 259:774–791.

Catazano, F., C. Giancola, G. Graziano, and G. Barone. 1996. Temperature-induced denaturation of ribonuclease S: a thermodynamic study. *Biochemistry.* 35:13378–13385.

Chakshusmati, G., G. S. Ratnaparkhi, P. K. Madhu, and R. Varadarajan. 1999. Native-state hydrogen-exchange studies of a fragment complex can provide structural information about the isolated fragments. *Proc. Natl. Acad. Sci. U. S. A.* 96:7899–7904.

Gilmanshin, R., J. Van Beek, and R. H. Callender. 1996. Study of the ribonuclease S-peptide/S-protein complex by means of Raman difference spectroscopy. *J. Phys. Chem.* 100:16755–16760.

Goldberg, J. M., and R. L. Baldwin. 1998. Kinetic mechanism of a partial folding reaction: 2. Nature of the transition state. *Biochemistry.* 37: 2556–2563.

Goldberg, M. S., J. Zhang, S. Sondek, C. R. Matthews, R. O. Fox, and A. L. Horwich. 1997. Native-like structure of a protein-folding intermediate bound to the chaperonin GroEl. *Proc. Natl. Acad. Sci. U. S. A.* 94:1080–1085.

Goux, W. J., and T. M. J. Hooker. 1980. Chiroptical properties of proteins: 1. Near-ultraviolet circular dichroism of ribonuclease S. *J. Am. Chem. Soc.* 102:7080–7087.

Graziano, G., F. Catazano, C. Giancola, and G. Barone. 1996. DSC study of the thermal stability of S-protein and S-peptide/S-protein complexes. *Biochemistry.* 35:13386–13392.

Haris, P. I., D. C. Lee, and D. Chapman. 1986. A Fourier transform infrared investigation of the structural differences between ribonuclease A and ribonuclease S. *Biochim. Biophys. Acta.* 874:255–265.

Hearn, R. P., F. M. Richards, J. M. Sturtevant, and G. D. Watt. 1971. Thermodynamics of the binding of S-peptide to S-protein to form ribonuclease S′. *Biochemistry.* 10:806–817.

Horwitz, J., and E. H. Strickland. 1971. Absorption and circular dichroism spectra of ribonuclease-S at 77°K. *J. Biol. Chem.* 246:3749–3752.

Keiderling, T. A. 2000. Peptide and protein conformational studies with vibrational circular dichroism and related spectroscopies. *In* Circular Dichroism: Principles and Applications. N. Berova, K. Nakanishi, and R. W. Woody, editors. Wiley, New York. 621–666.

Kim, E. E., R. Vadarajan, H. W. Wyckoff, and F. M. Richards. 1992. Refinement of the crystal structure of ribonuclease S: comparison with and between the various ribonuclease A structures. *Biochemistry.* 31: 12304–12314.

Klee, W. A. 1968. Studies of the conformation of ribonuclease S-peptide. *Biochemistry.* 8:2731–2736.

Kurapkat, G., P. Kruger, A. Wollmer, J. Fleischhauer, B. Kramer, E. Zobel, A. Koslowski, H. Botterweck, and R. W. Woody. 1997. Calculations of the CD spectrum of bovine pancreatic ribonuclease. *Biopolymers.* 41: 267–287.

Labhardt, A. 1982. Secondary structure in ribonuclease: I. Equilibrium folding transitions seen by amide circular dichroism. *J. Mol. Biol.* 157:331–355.

Labhardt, A. M. 1981. An equilibrium folding intermediate detected in the thermal unfolding of ribonuclease S by circular dichroism. *Biopolymers.* 20:1450–1480.

Labhardt, A. M., and R. L. Baldwin. 1979. Recombination of S-peptide with S-protein during folding of ribonuclease S: I. Folding pathways of the slow-folding and fast-folding classes of unfolded S-protein. *J. Mol. Biol.* 135:231–244.

Lumry, R., R. Biltonen, and J. Brandts. 1966. Validity of the "two-state" hypothesis for conformational transitions of proteins. *Biopolymers.* 4:917–944.

Makhatadze, G. I., G. M. Clore, and A. M. Gronenborn. 1995. Solvent isotope effect and protein stability. *Nat. Struct. Biol.* 2:852–855.

Malinowski, E. R. 1991. Factor Analysis in Chemistry. Wiley, New York.

Pancoska, P., E. Bitto, V. Janota, and T. A. Keiderling. 1994. Quantitative analysis of vibrational circular dichroism spectra of proteins: problems and perspectives. *Faraday Discuss.* 99:287–310.

Pancoska, P., E. Bitto, V. Janota, M. Urbanova, V. P. Gupta, and T. A. Keiderling. 1995. Comparison of and limits of accuracy for statistical analyses of vibrational and electronic circular dichroism spectra in terms of correlations to and predictions of protein secondary structure. *Protein Sci.* 4:1384–1401.

Pancoska, P., S. C. Yasui, and T. A. Keiderling. 1991. Statistical analysis of the vibrational circular dichroism of selected proteins and relationship to secondary structures. *Biochemistry.* 30:5089–5103.

Richards, F. M., and P. J. Vithayathil. 1959. The preparation of subtilisin-modified ribonuclease and the separation of the peptide and protein components. *J. Biol. Chem.* 234:1459–1465.

Rico, M., M. Bruix, J. Santoro, C. Gonzales, J. L. Neira, J. L. Nieto, and J. Herranz. 1989. Sequential ^{1}H-NMR assignment and solution structure of bovine pancreatic ribonuclease A. *Eur. J. Biochem.* 183:623–638.

Schreier, A. A., and R. L. Baldwin. 1976. Concentration-dependent hydrogen exchange kinetics of ^{3}H-labeled S-peptide in ribonuclease S. *J. Mol. Biol.* 105:409–426.

Schreier, A. A., and R. L. Baldwin. 1977. Mechanism of dissociation of S-peptide from ribonuclease S. *Biochemistry.* 16:4203–4209.

Sela, M., and C. B. Anfinsen. 1957. Some spectrometric and polarimetric experiments with ribonuclease. *Biophys. Biochim. Acta.* 24:229–235.

Seshadri, S., K. A. Oberg, and A. L. Fink. 1994. Thermally denatured ribonuclease A retains secondary structure as shown by FTIR. *Biochemistry.* 33:1351–1355.

Sherwood, L. M., and J. T. J. Potts. 1965. Conformational studies of pancreatic ribonuclease and its subtilisin-produced derivatives. *J. Biol. Chem.* 240:3799–3805.

Shindo, H., S. Matsuura, and J. S. Cohen. 1979. Conformation of ribonuclease S-protein. *Experientia.* 35:1284–1285.

Simons, E. R., E. G. Schneider, and E. R. Blout. 1969. Thermal effects on the circular dichroism spectra of ribonuclease A and of ribonuclease S-protein. *J. Biol. Chem.* 244:4023–4026.

Sosnick, T. R., and J. Trewhella. 1992. Denatured states of ribonuclease A have compact dimensions and residual secondary structure. *Biochemistry.* 31:8329–8335.

Stelea, S., P. Pancoska, and T. A. Keiderling. 2001. Thermal unfolding of ribonuclease A in phosphate at neutral pH: deviations from the two state model. *Protein Sci.* 10:970–978.

Strickland, E. H. 1972. Interactions contributing to the tyrosyl circular dichroism bands of ribonuclease S and A. *Biochemistry.* 11:3465–3474.

Vadarajan, R., and F. M. Richards. 1992. Crystallographic structures of ribonuclease S variants with nonpolar substitution at position 13: packing and cavities. *Biochemistry.* 31:12315–12327.

Wang, L. 1993. Vibrational circular dichroism studies of nucleic acid conformations. Ph.D. thesis. University of Illinois at Chicago, Chicago, Illinois. 264 pp.

Wlodawer, A., R. Bott, and L. Sjolin. 1982. The refined crystal structure of ribonuclease A at 2.0 A resolution. *J. Biol. Chem.* 257:1325–1332.

Wyckoff, H. W., D. Tsernoglou, A. W. Hanson, J. R. Knox, B. Lee, and F. M. Richards. 1970. The three-dimensional structure of ribonuclease-S: interpretation of an electron density map at a nominal resolution of 2 A. *J. Biol. Chem.* 245:305–328.